Supporting Information

Oxamusplatin: A cytotoxic Pt(II) complex of a nitrogen mustard with resistance to thiol based sequestration display enhanced selectivity to cancer cells

Moumita Maji‡ [a], Subhendu Karmakar‡ [a], Ruturaj [b], Arnab Gupta [b], Arindam Mukherjee* [a]

[a]Department of Chemical Sciences and Centre for Advanced Functional Materials, Indian Institute of Science Education and Research Kolkata
Mohanpur-741246, West Bengal, India

[b]Department of Chemical Sciences Indian Institute of Science Education and Research Kolkata
Mohanpur-741246, West Bengal, India

Corresponding author. E-mail: a.mukherjee@iiserkol.ac.in

Fax: (+91)033-25873118; Tel: (+91)033-25873121;

‡These authors contributed equally

Contents

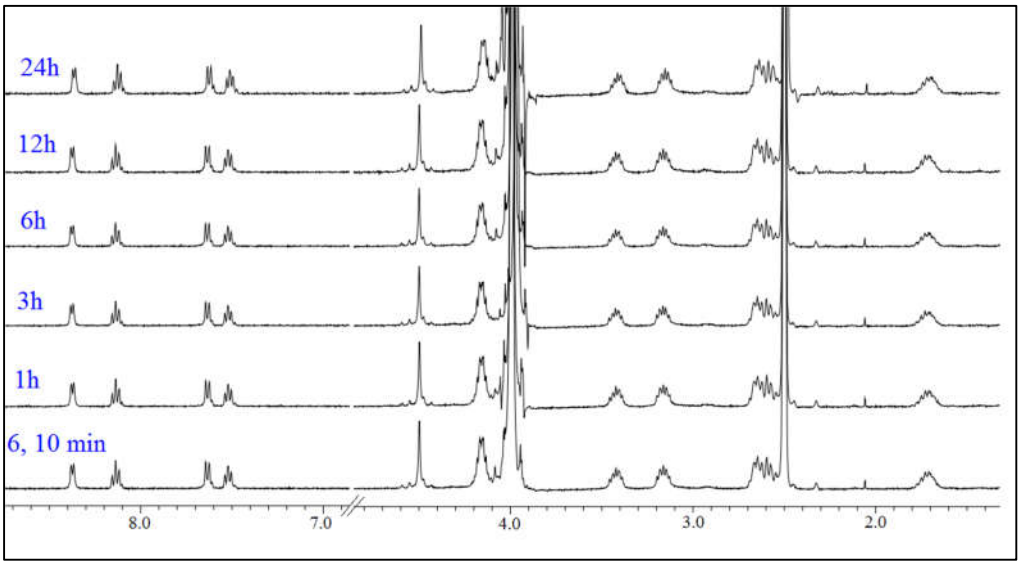

Figure S1. Stability study of complex **6** in 50% 20 mM phosphate buffer in DMSO-d_6 (pD 7.4, 4mM NaCl), monitored by ^{1}H NMR data suggests that there is no hydrolysis.

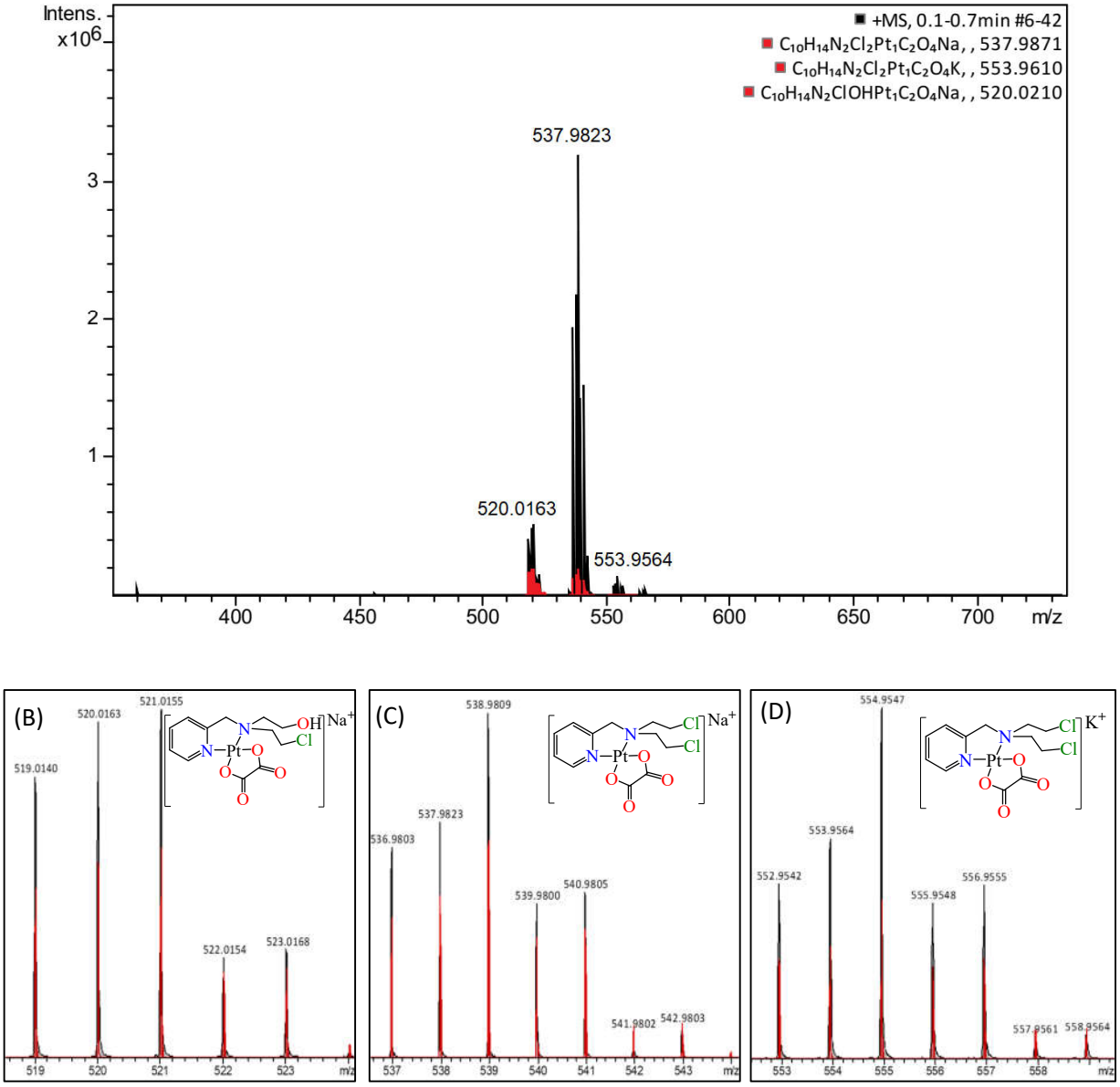

Figure S2. ESI-MS spectra of hydrolysis of oxamusplatin after 10 min incubation in 50% 5 mM phosphate buffer (pH 7.4, 4 mM NaCl) and MeOH mixture shows there is no hydrolysis: overall speciation (A) isotopic distribution of the complex where one of the chlorine from the nitrogen mustard is hydrolyzed depicting *m/z* 520.016 (Calc: 520.021) (B); intact oxamusplatin with sodium ion having *m/z* 537.982 (Calc: 537.987) (C) and potassium ion with *m/z* 553.956 (Calc: 553.961) (D).

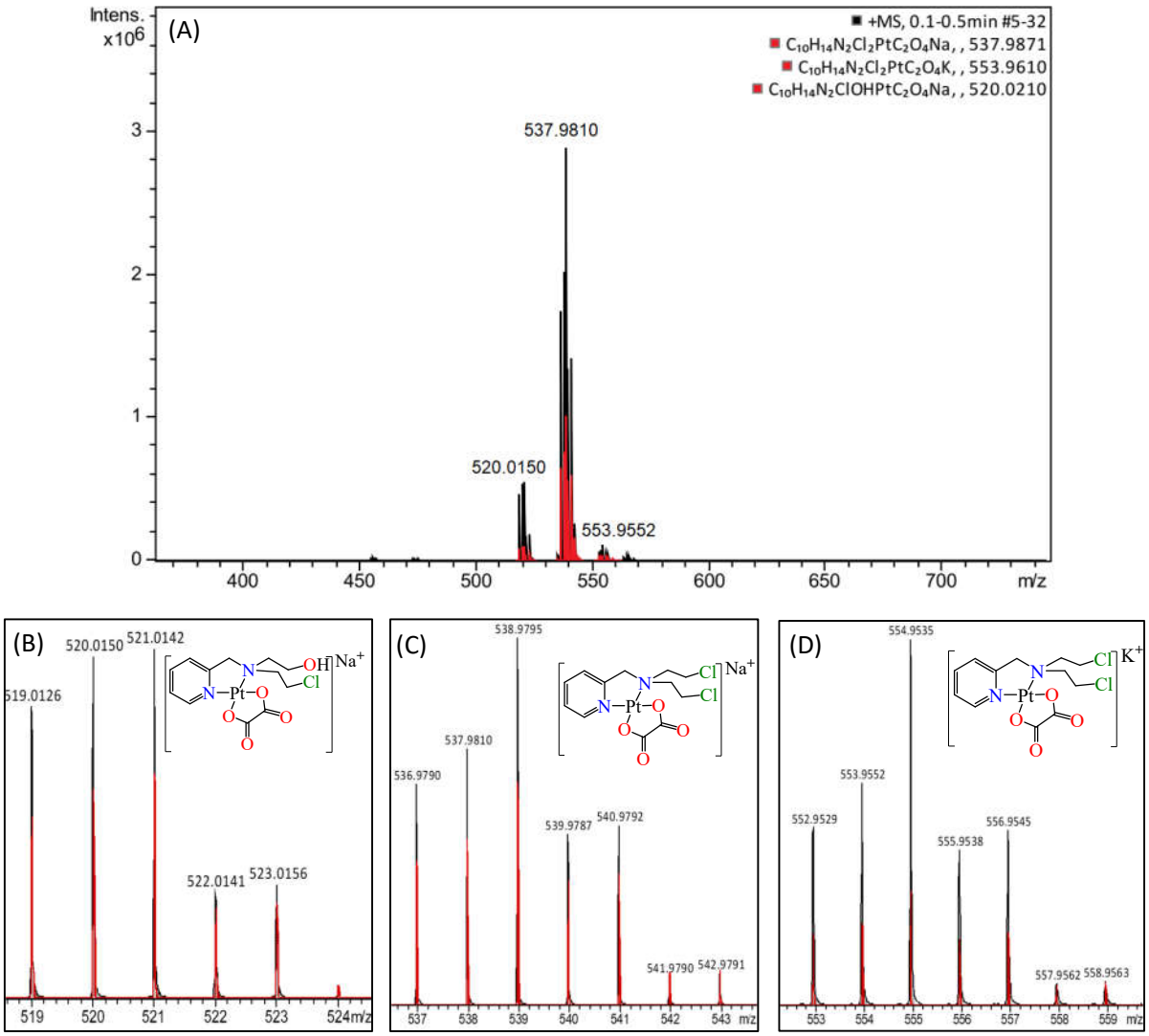

Figure S3. ESI-MS spectra of hydrolysis of oxamusplatin after 24 h incubation in 50% 5 mM phosphate buffer (pH 7.4, 4 mM NaCl) in MeOH mixture shows there is no hydrolysis: overall speciation (A); isotopic distribution of the complex where one of the chlorine from the nitrogen mustard is hydrolyzed depicting *m/z* 520.015 (Calc: 520.021) (B); intact oxamusplatin with sodium ion having *m/z* 537.981 (Calc: 537.987) (C) and potassium ion with *m/z* 553.955 (Calc: 553.961) (D).

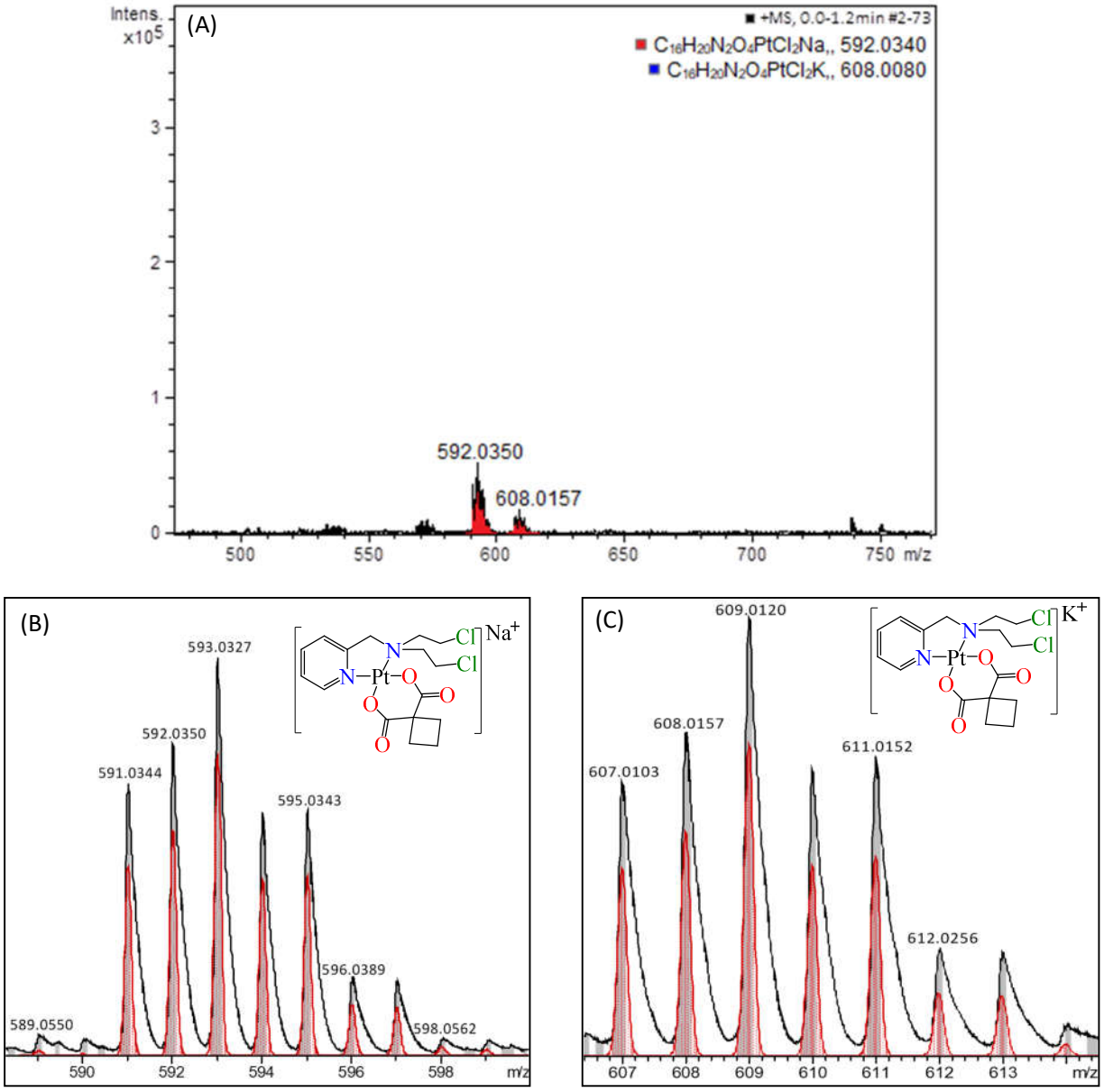

Figure S4. ESI-MS spectra of hydrolysis of **6** after 24 h incubation in 50% 5 mM phosphate buffer (pH 7.4, 4 mM NaCl) in MeOH mixture exhibiting that there is no hydrolysis: overall speciation (A); isotopic distribution of intact **6** with sodium ion having *m/z* 592.035 (Calc: 592.034) (B); and potassium ion with *m/z* 608.015 (Calc: 608.008) (C).

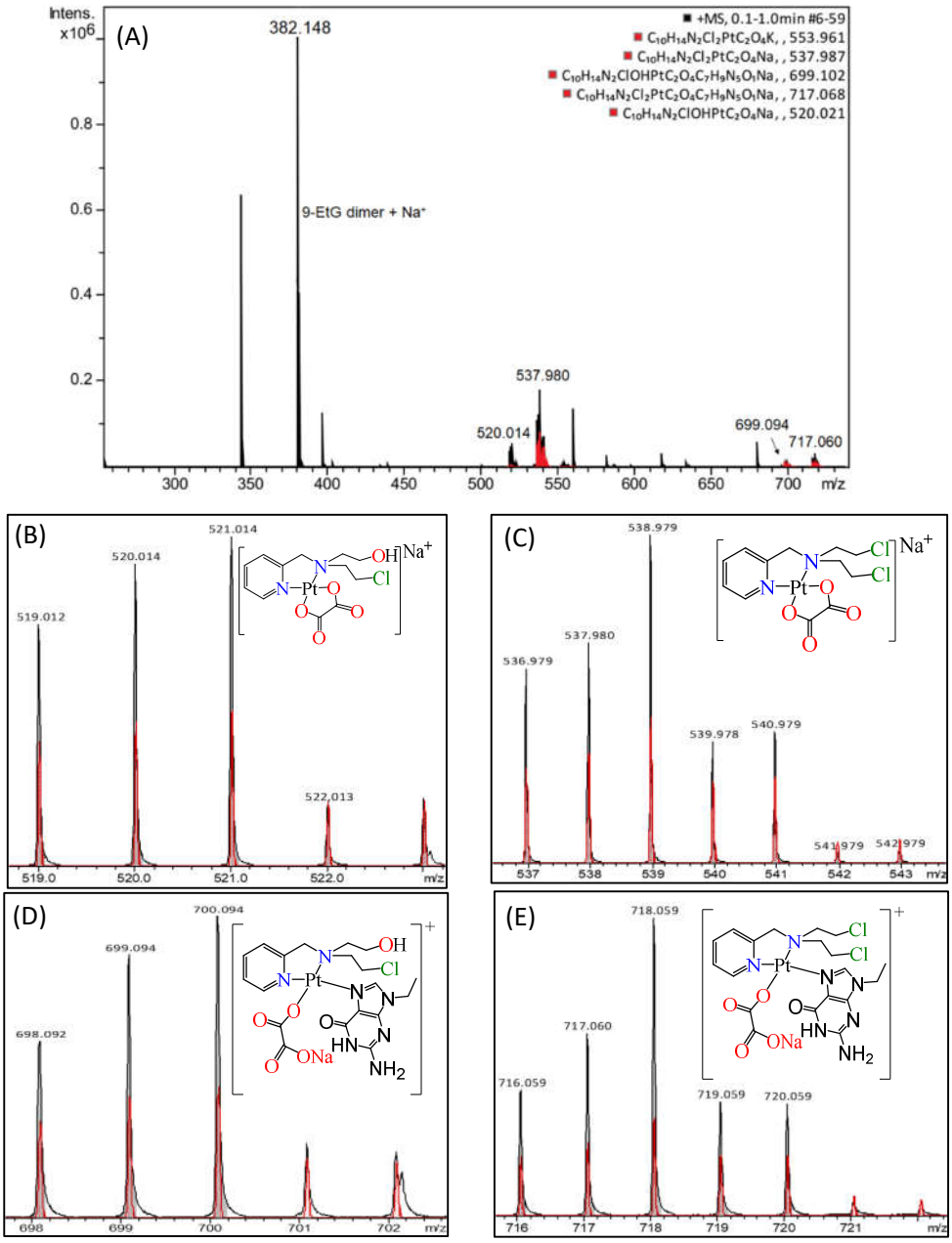

Figure S5. ESI-MS spectra of 9-ethylguanine (9-EtG) interaction with oxamusplatin after incubation for 12 h with 5 mol equivalents of 9-EtG in 50% 5 mM phosphate buffer (pH 7.4, 4 mM NaCl) in MeOH mixture displaying intact complex and formation of 9-EtG adduct: overall speciation (A); isotopic distribution of the complex where one of the chlorine from the nitrogen mustard is hydrolyzed depicting *m/z* 520.014 (Calc: 520.021) (B); the intact complex with *m/z* 537.980 (Calc: 537.987) (C);9-EtG mono adduct of the species where one chloro from the nitrogen mustard is hydrolyzed depicting *m/z* 699.094 (Calc: 699.102) (C). 9-EtG mono adduct of oxamusplatin with *m/z* 717.060 (Calc: 717.068) (D).

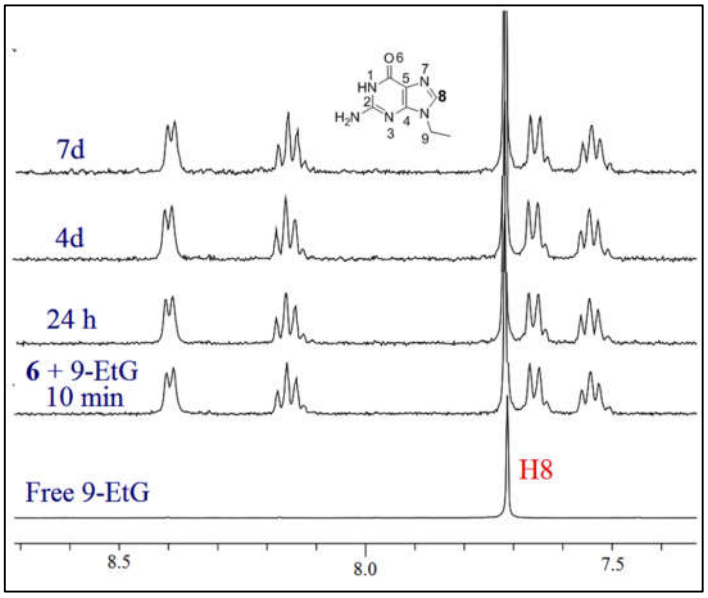

Figure S6. ^{1}H NMR data of **6** with 3 mol equivalents of 9-EtG in 50% 20 mM phosphate buffer in DMSO-d_6 (pD 7.4). Data suggests that there is no binding between **6** and 9-EtG.

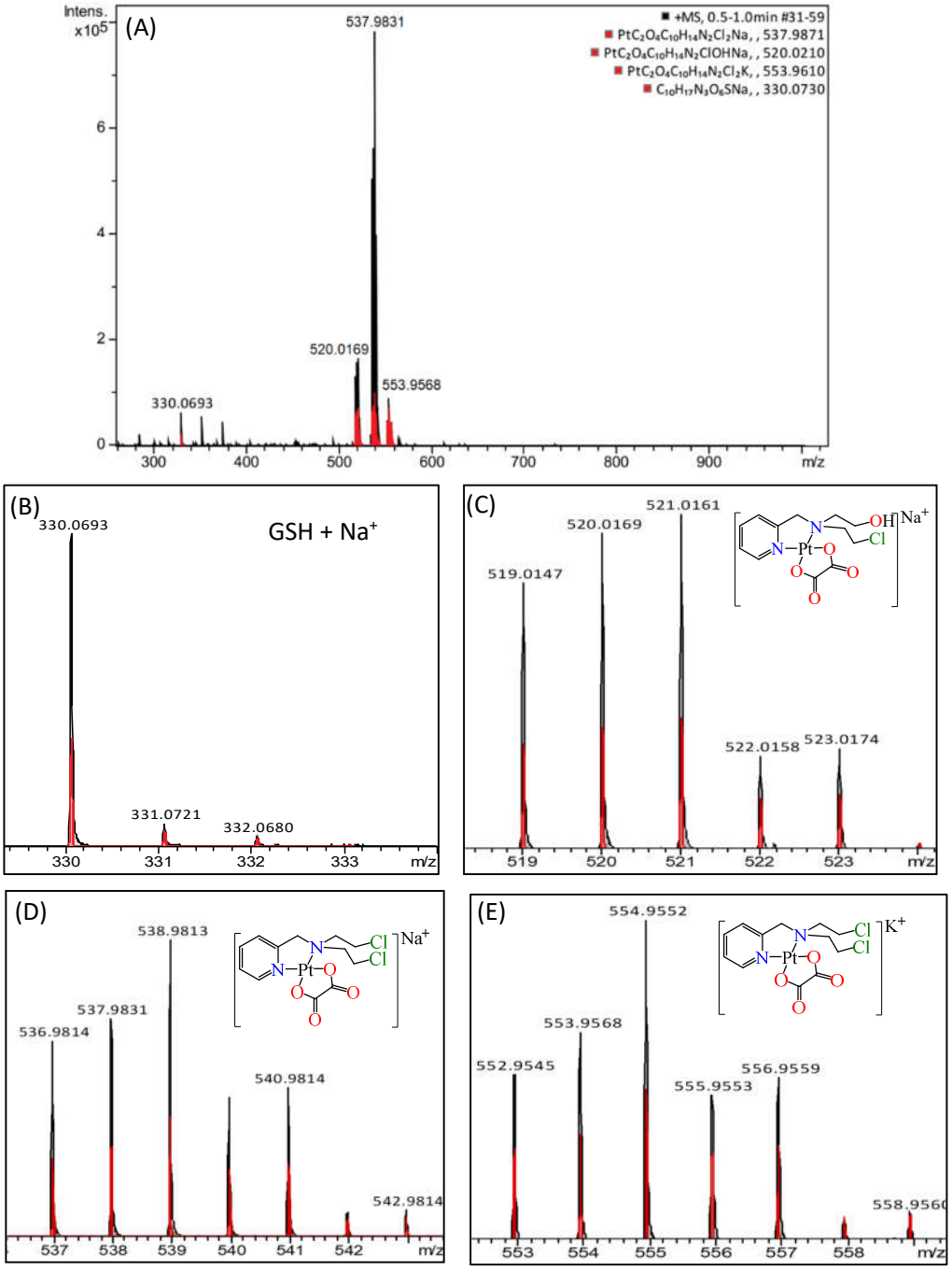

Figure S7. ESI-MS spectra of Glutathione (GSH) interaction with oxamusplatin showing no adduct formation even after 24 h incubation with 3 mol equivalents of GSH in 50% 5 mM phosphate buffer (pH 7.4, 4 mM NaCl) in MeOH mixture: overall speciation (A); isotopic distribution of GSH with sodium ion (B); the complex where one of the chlorine from the nitrogen mustard is hydrolyzed depicting *m/z* 520.017 (Calc: 520.021) (C); intact oxamusplatin with sodium ion having *m/z* 537.983 (Calc: 537.987) (D) and potassium ion with *m/z* 553.957 (Calc: 553.961) (E).

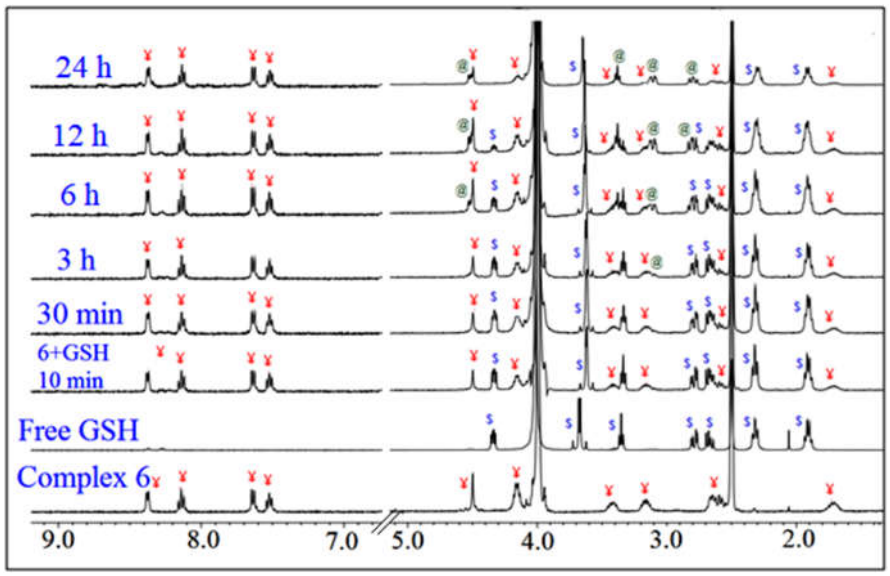

Figure S8. ^{1}H NMR data of complex **6** showing it does not bind GSH only auto-oxidation of GSH with time observed. 3 mol equivalents of GSH was used in 1: 1 (v/v) phosphate buffer (20 mM, pD 7.4 containing 4mM NaCl): DMSO-d_6. Where, '¥' intact complex **6**; '$' free GSH; '@' GSH dimer due to auto-oxidation.

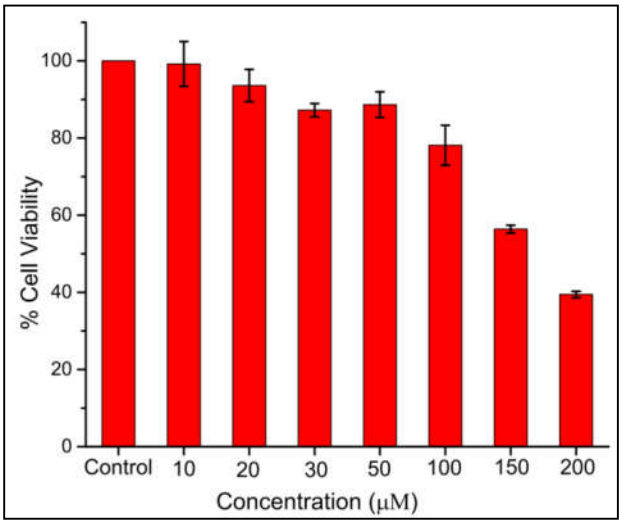

Figure S9. Percentage of cell viability of different concentration (μM) of oxamusplatin in normal human foreskin fibroblast cell line HFF-1.

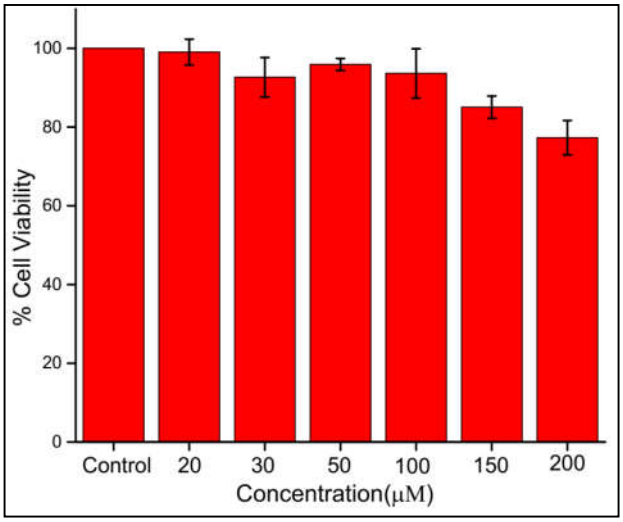

Figure S10. Percentage of cell viability of different concentration (μM) of oxamusplatin in non-cancerous canine kidney cell line (MDCK).

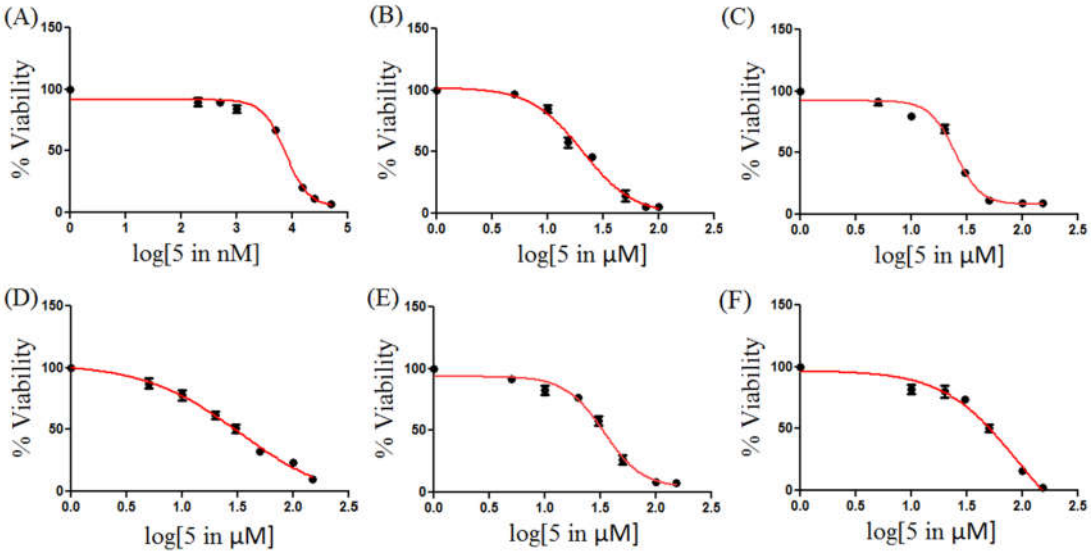

Figure S11. Plots of cell viability (%) vs. log of concentrations of oxamusplatin (**5**) against (A) MCF-7, (B) DU-145, (C) MIA PaCa-2, (D) Hep G2, (E) PANC-1 and (F) CHO cell lines after incubation for 72 h determined from MTT assays under normoxic condition. The plots provided are for one independent experiment out of at least three independent experiments.

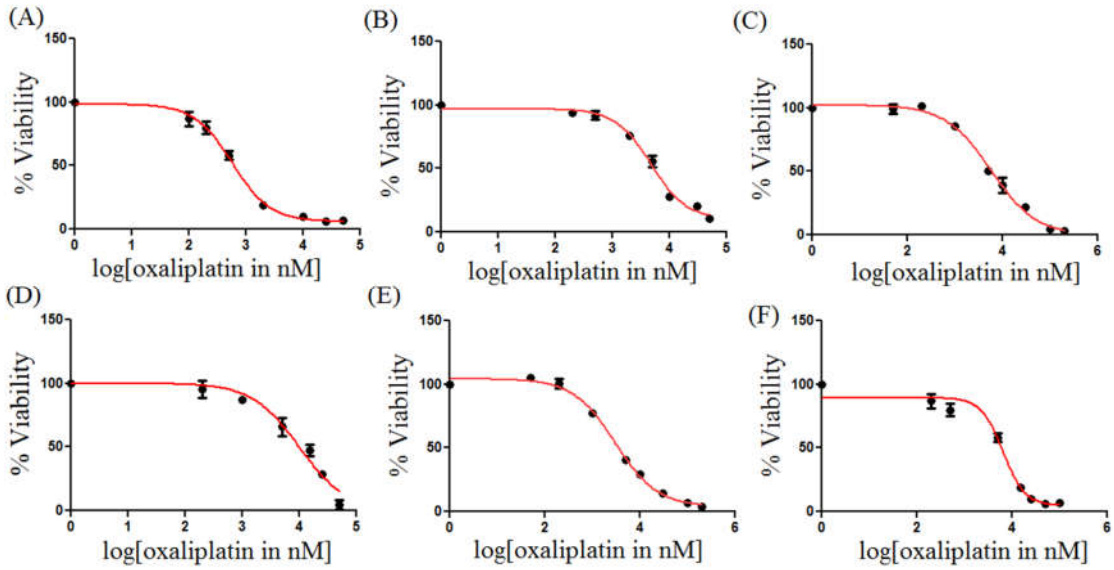

Figure S12. Plots of cell viability (%) vs. log of concentrations of oxaliplatin against (A) MCF-7, (B) DU-145, (C) MIA PaCa-2, (D) Hep G2, (E) PANC-1 and (F) HFF-1 cell lines after incubation for 72 h determined from MTT assays under normoxic condition. The plots provided are for one independent experiment out of at least three independent experiments.

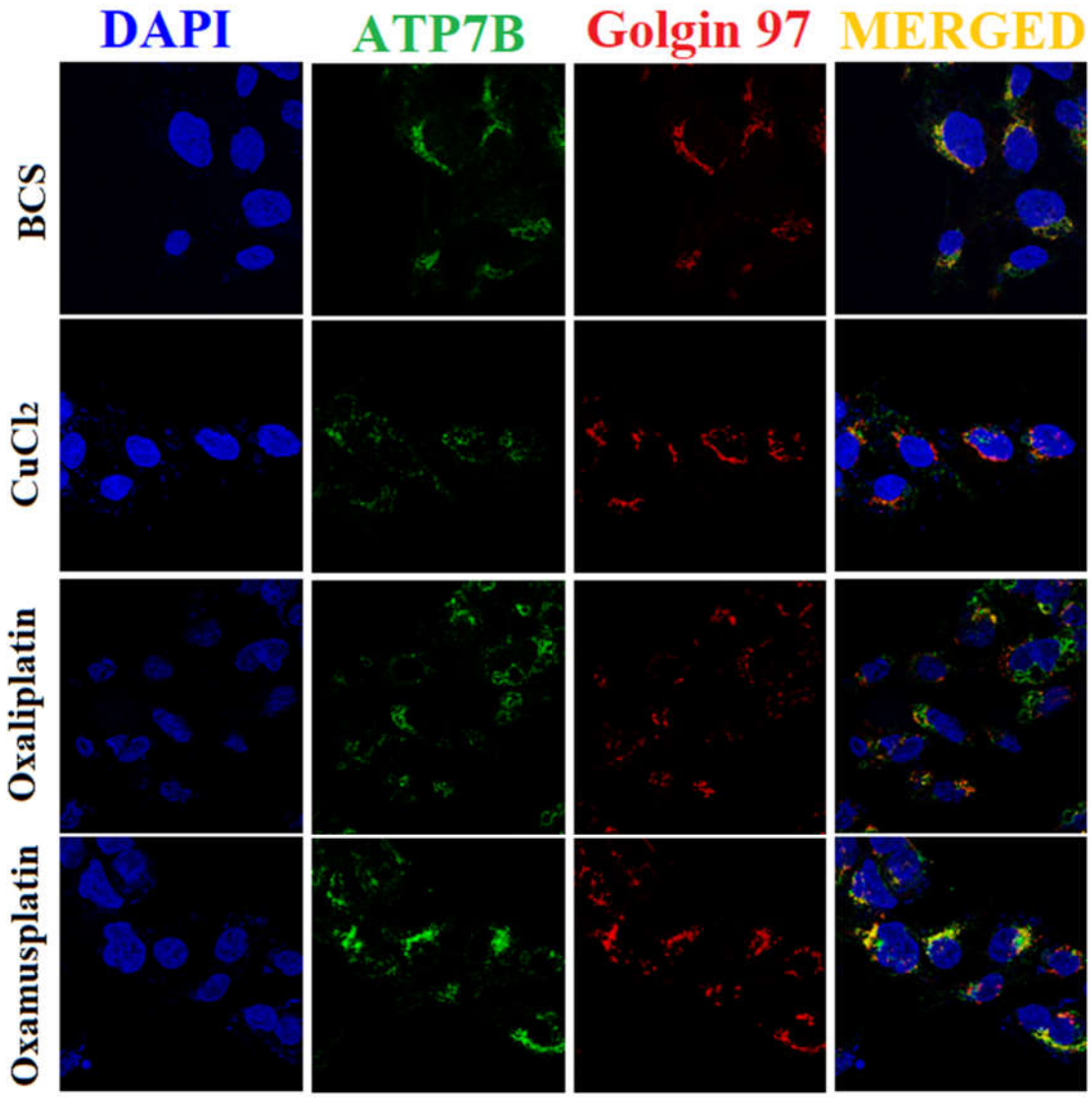

Figure S13. Immunofluorescence studies in Hep G2 cells showing the mobilization of ATP7B from the *trans*-golgi network (TGN) upon administration of the copper chelator bathocuproinedisulfonate (BCS) (50 µM), $CuCl_2$ (50 µM), oxaliplatin (20 µM) and oxamusplatin (20 µM). In case of BCS and oxamusplatin the highest co-localization of the ATP7B in TGN is observed.

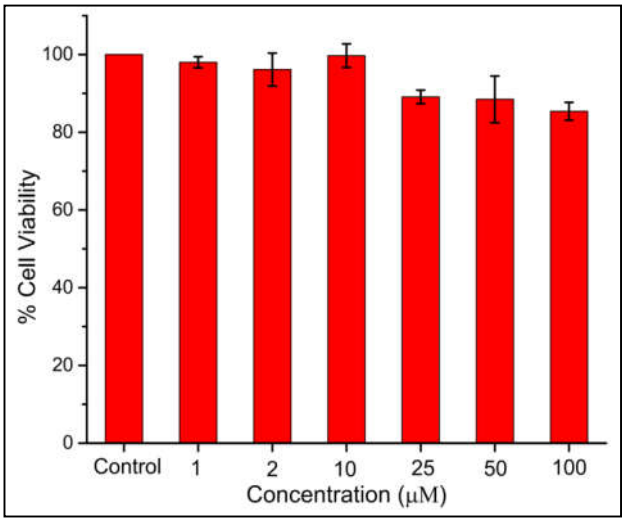

Figure S14. Percentage of cell viability in presence of different concentration (μM) of verapamil in DU-145 cell line.

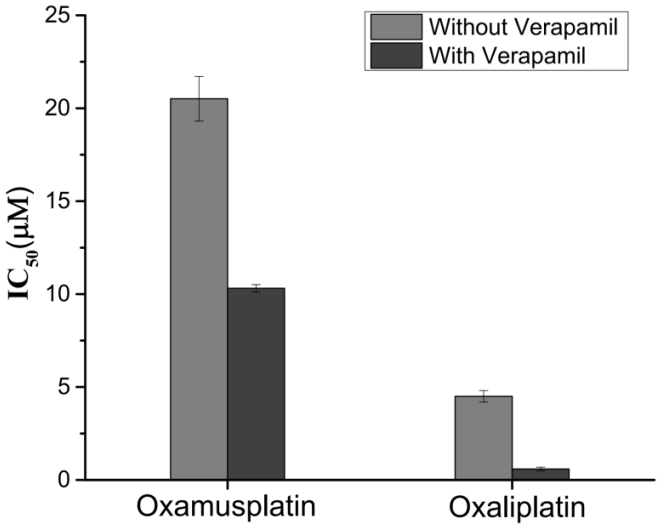

Figure S15. Effect of the P-gp inhibitor verapamil in increasing cytotoxicity, displaying oxamusplatin is less susceptible to P-gp transport compared to oxaliplatin

Table S1. Cytotoxicity of oxamusplatin and oxaliplatin in DU-145 in presence of 10 µM verapamil.

Complexes	IC_{50} ± SD (µM)
Oxamusplatin	10.32 ± 0.02
Oxaliplatin	0.597 ± 0.01

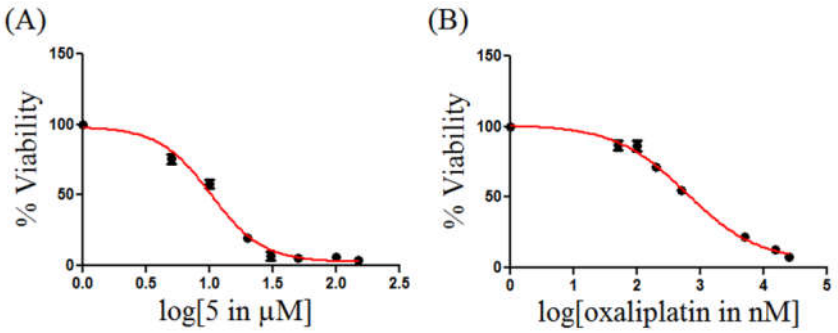

Figure S16. Plots of cell viability (%) vs. log of concentrations of (A) oxamusplatin (**5**) and (B) oxaliplatin against DU-145 in presence of 10 µM of verapamil after incubation for 72 h determined from MTT assays under normoxic condition. The plots provided are for one independent experiment out of at least three independent experiments

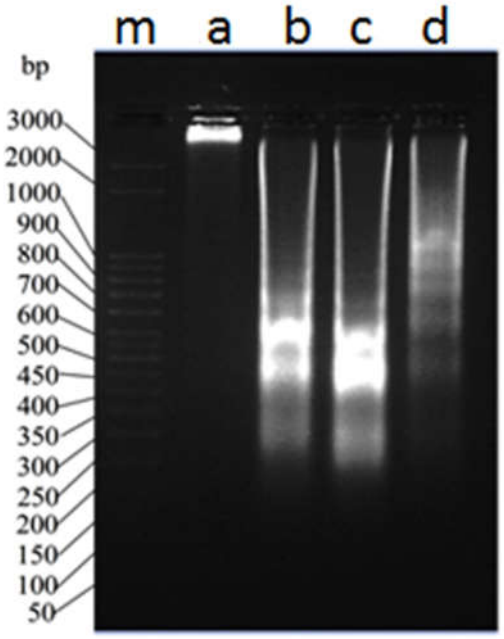

Figure S17. Gel image of DNA ladder formation using MCF-7 cells treated with different concentration of oxamusplatin (a) DMSO, (b) IC_{20}, (c) IC_{30} (d) IC_{50} over 24 h. 'm' denotes the standard base pair ladder.

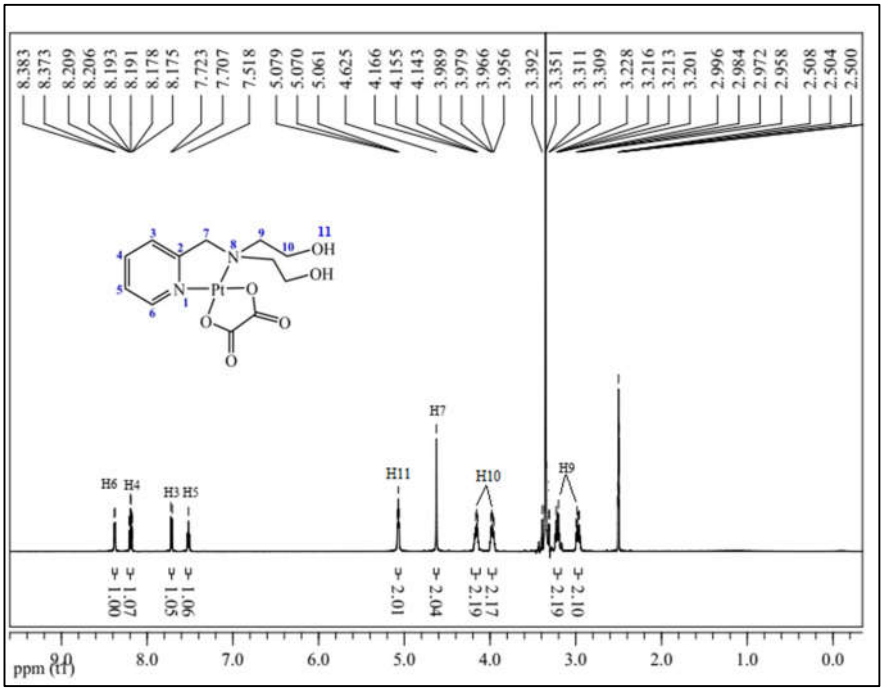

Figure S18. ^{1}H NMR of complex **3** in DMSO-d_6, 500 MHz.

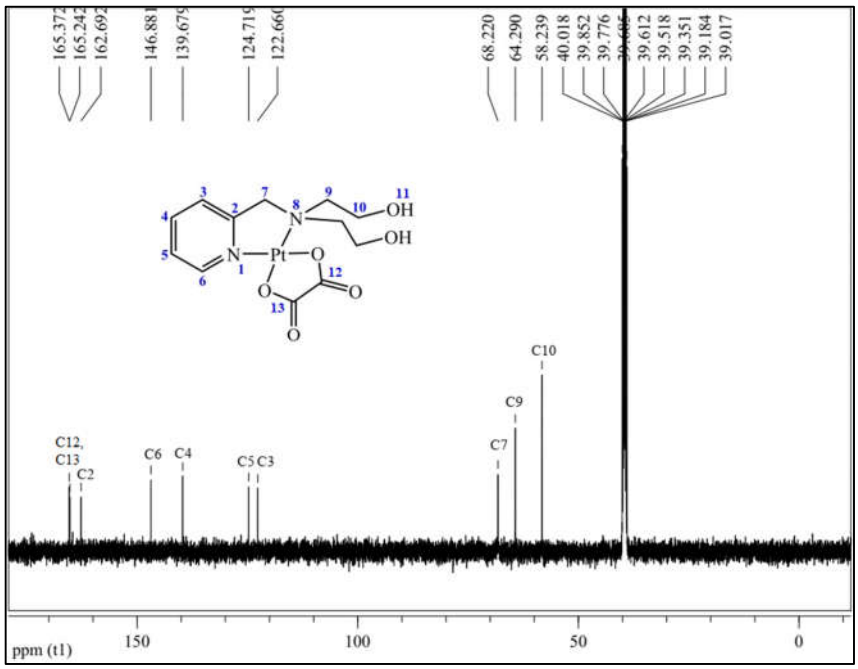

Figure S19. ^{13}C NMR of complex **3** in DMSO-d_6, 125 MHz.

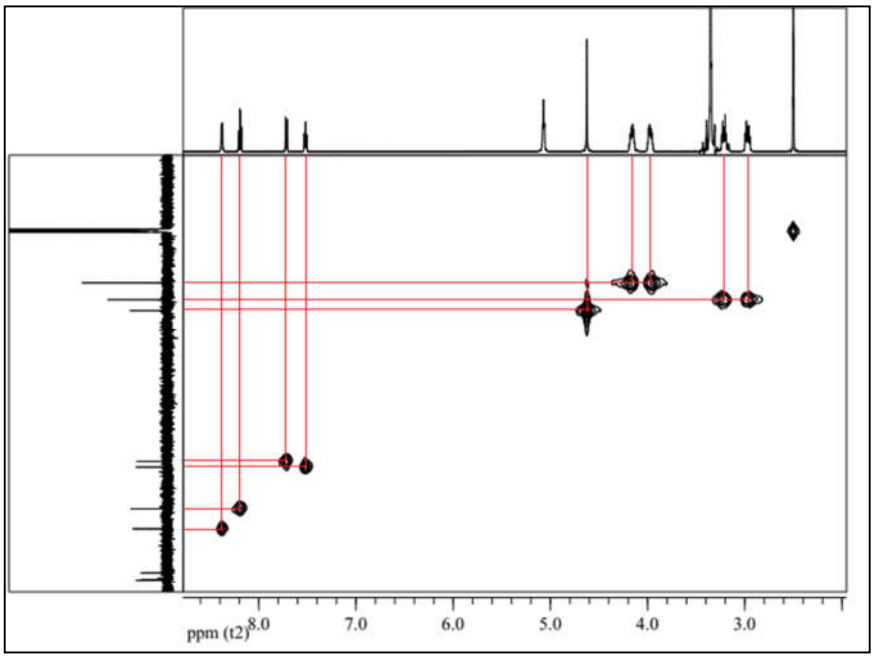

Figure S20. HMQC spectra of complex **3** in DMSO-d_6.

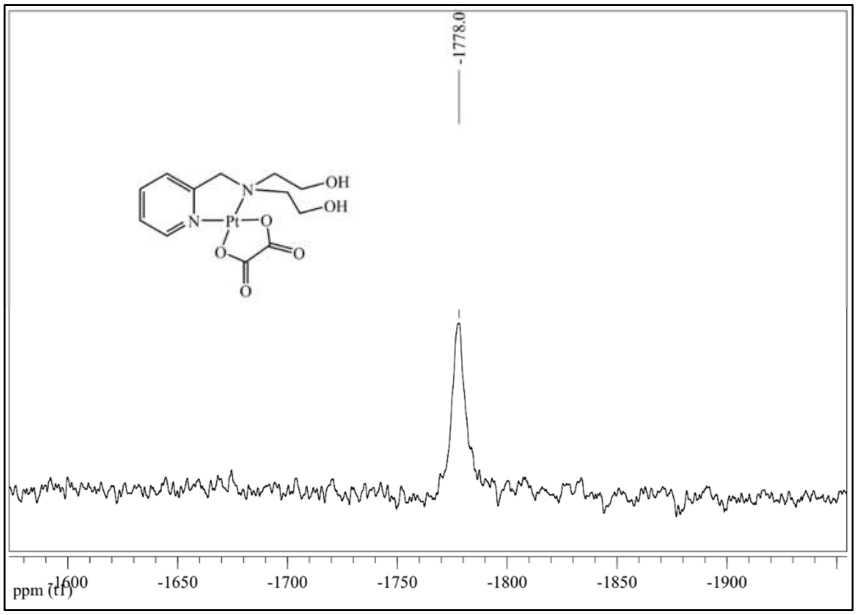

Figure S21. ^{195}PtNMR spectra of complex **3** in DMSO-d_6.

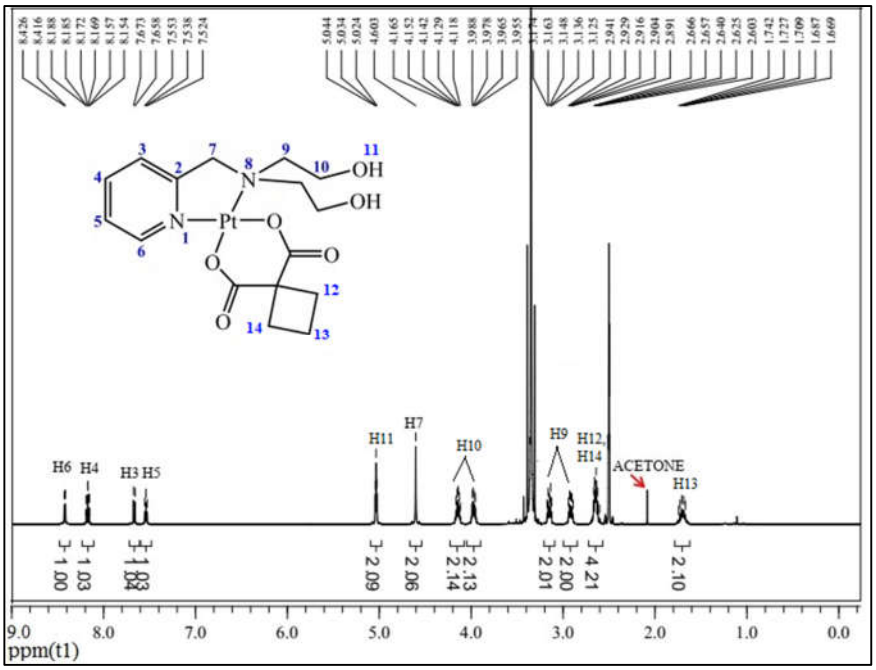

Figure S22. ^{1}H NMR of complex **4** in DMSO-d_6, 500 MHz.

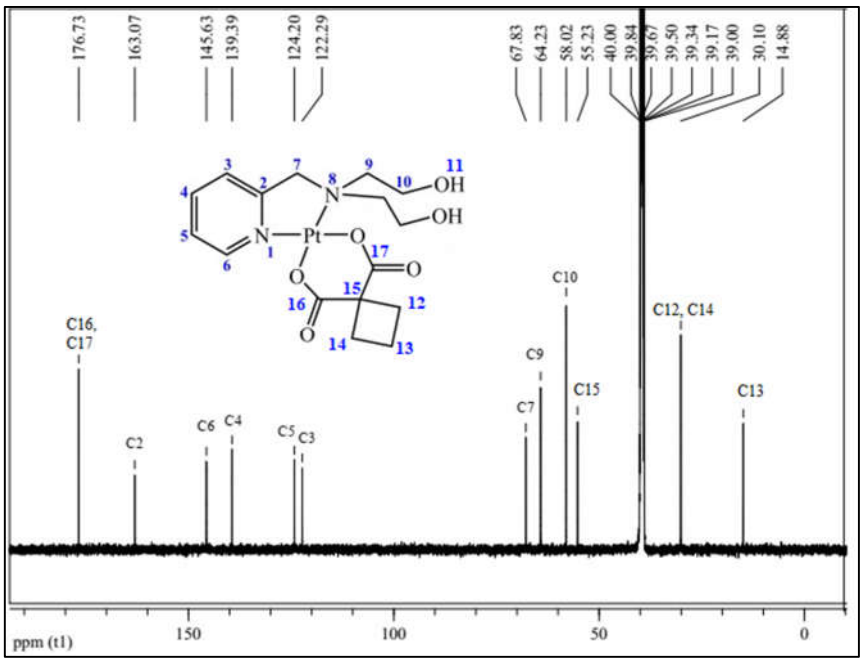

Figure S23. ^{13}C NMR of complex **4** in DMSO-d_6, 125 MHz.

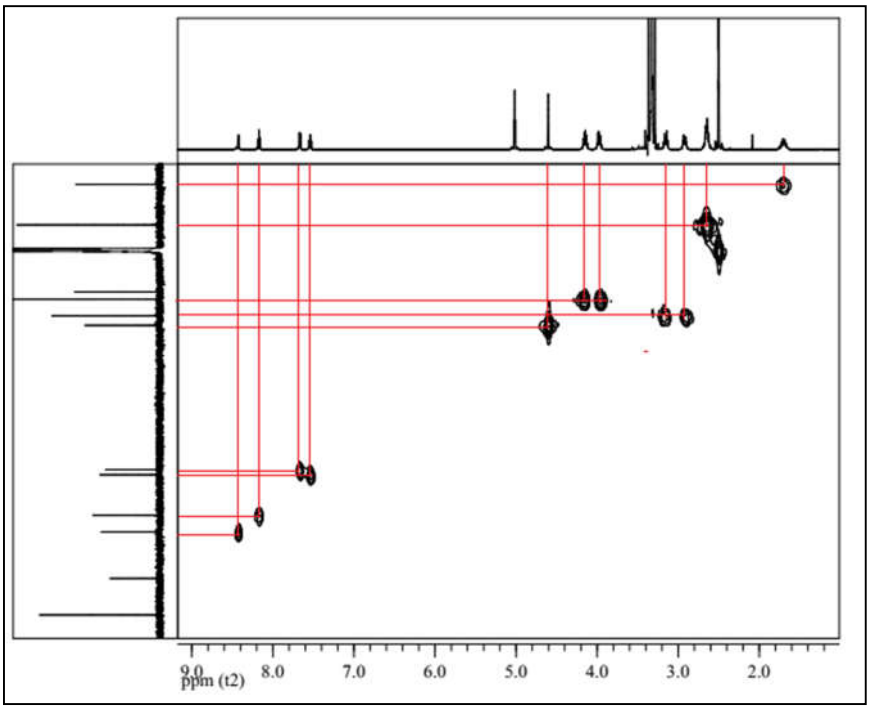

Figure S24. HMQC spectra of complex **4** in DMSO-d_6.

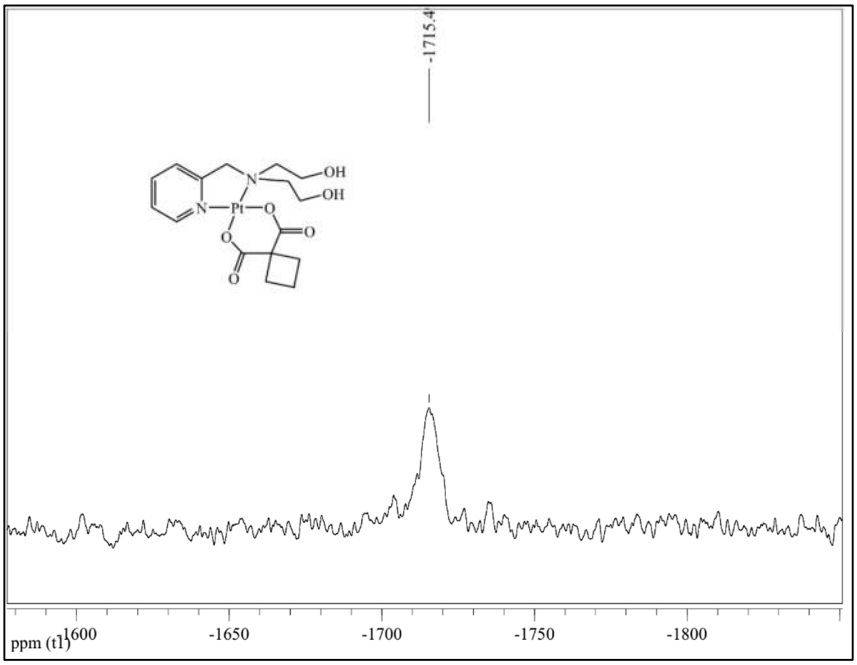

Figure S25. ^{195}PtNMR spectra of complex **4** in DMSO-d_6.

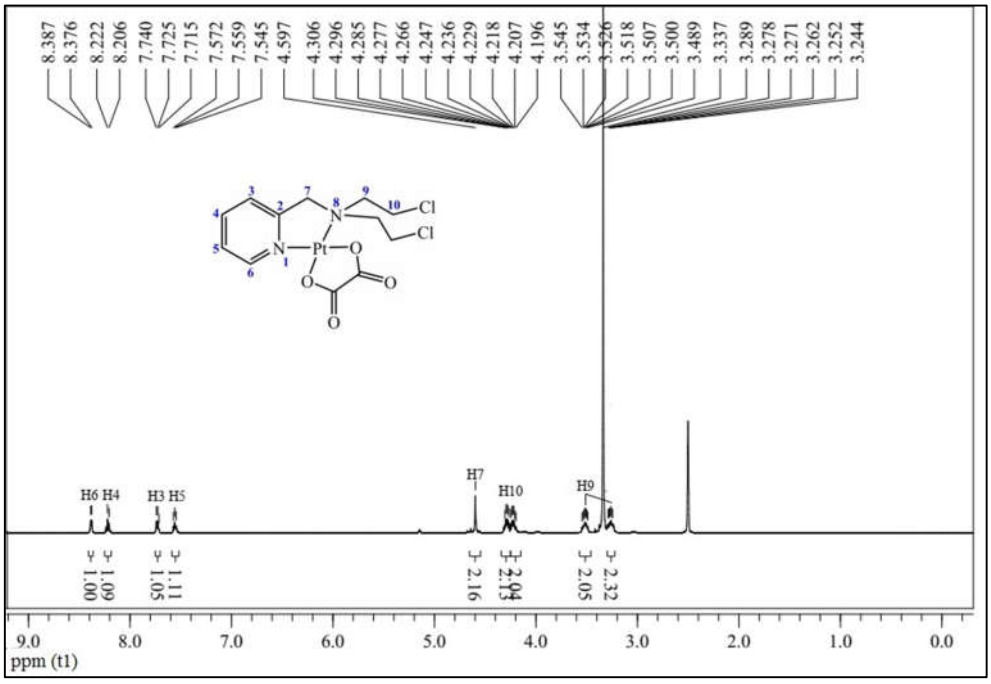

Figure S26. ^{1}H NMR of oxamusplatin in DMSO-d_6, 500 MHz.

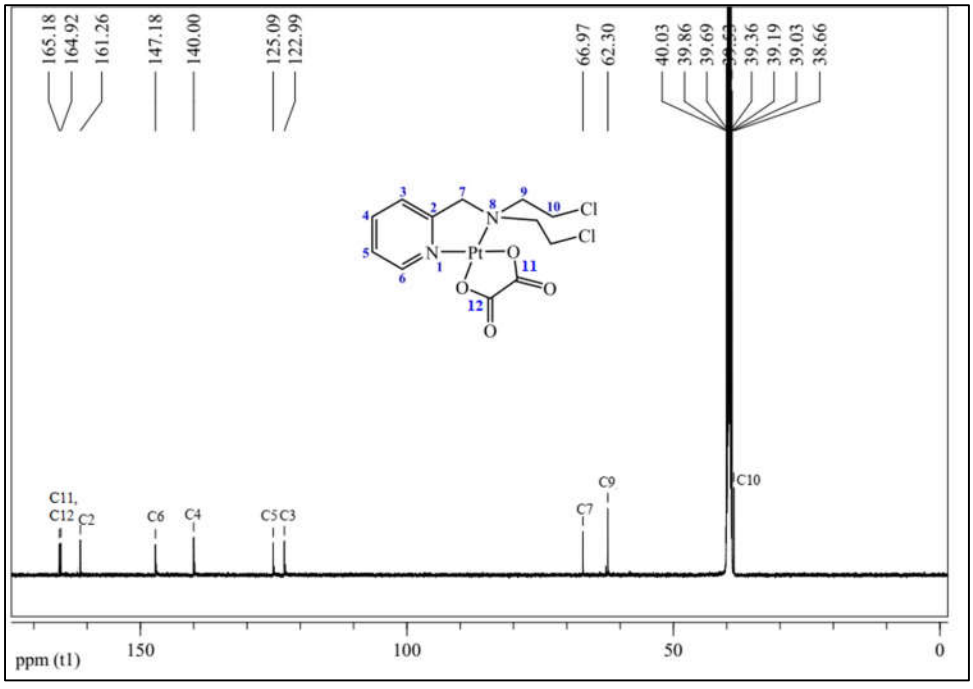

Figure S27. ^{13}C NMR of oxamusplatin in DMSO-d_6, 125 MHz.

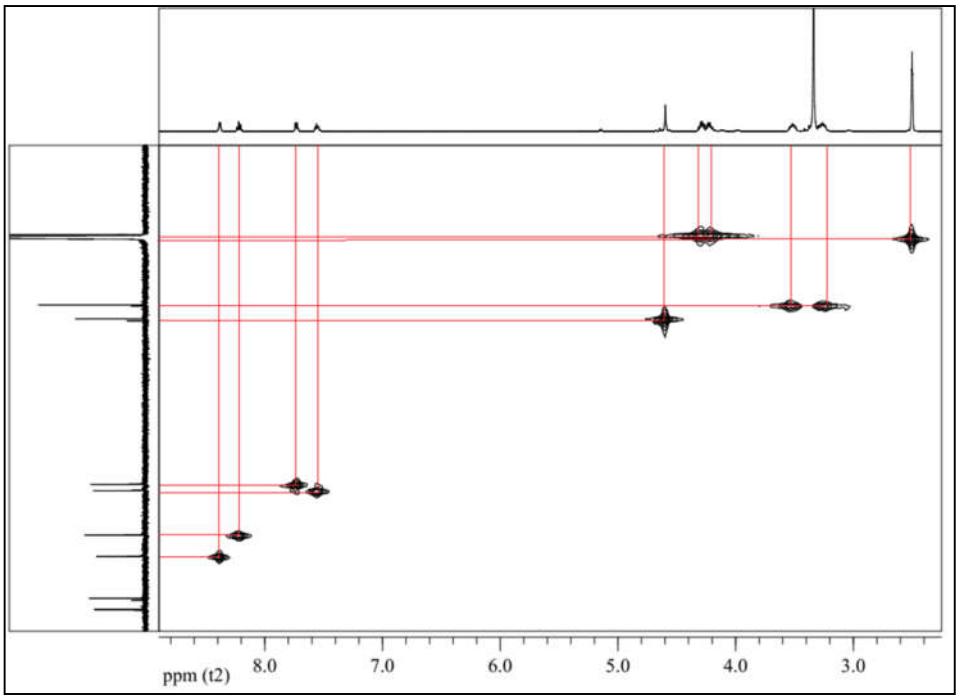

Figure S28. HMQC spectra of oxamusplatin in DMSO-d_6.

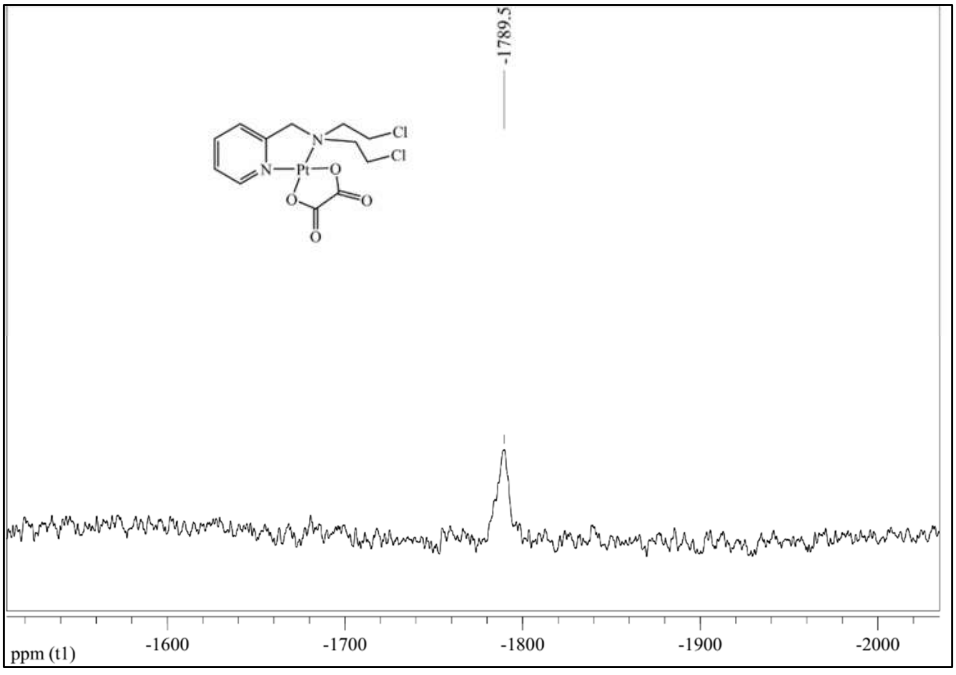

Figure S29. ^{195}PtNMR spectra of oxamusplatin in DMSO-d_6.

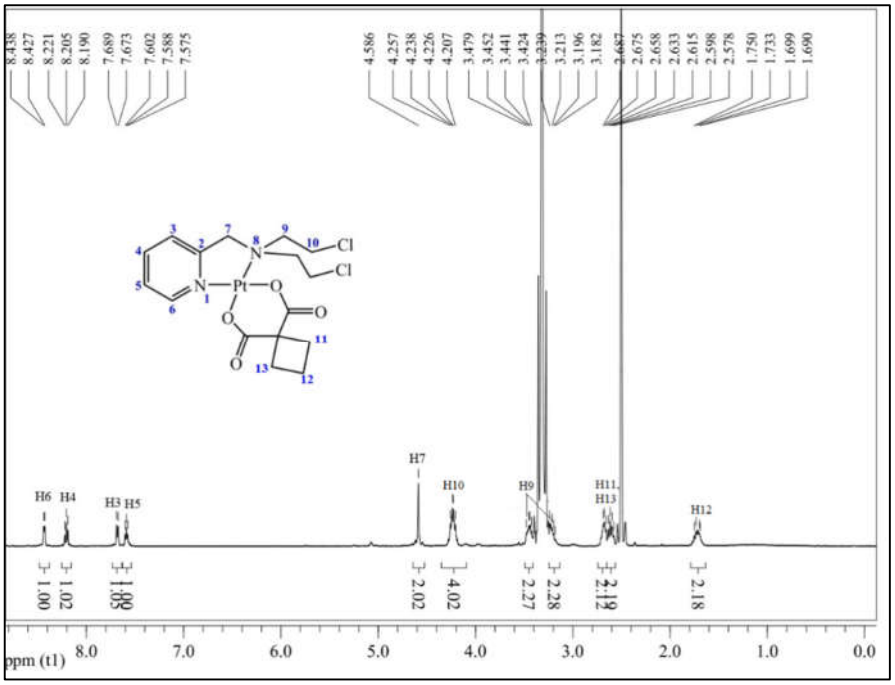

Figure S30. [1]H NMR of complex **6** in DMSO-d_6, 500 MHz.

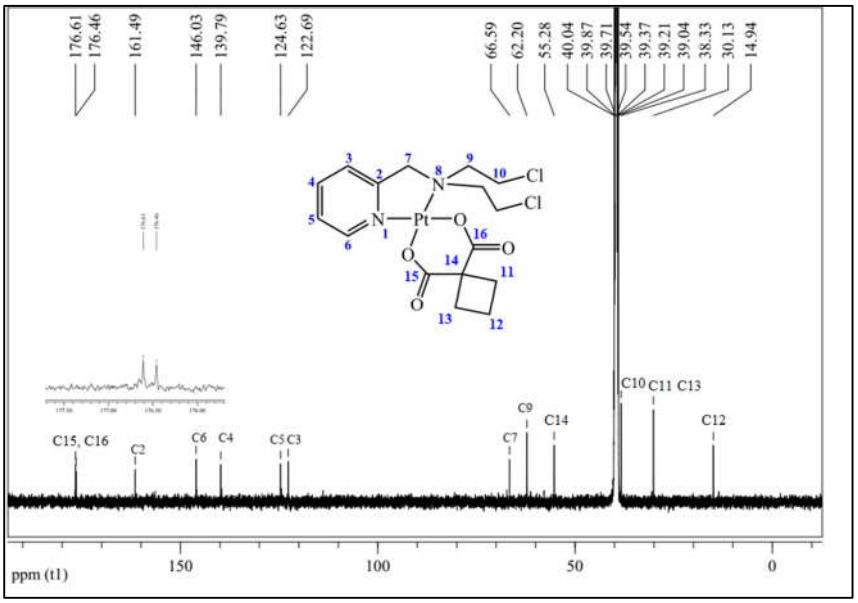

Figure S31.[13]C NMR of complex **6** in DMSO-d_6, 125 MHz.

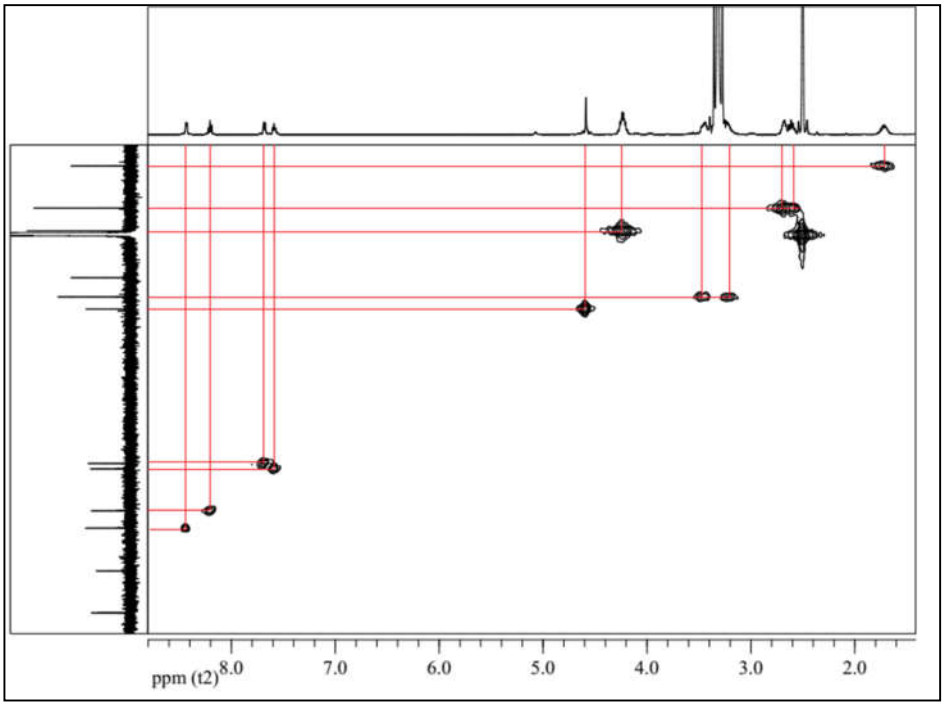

Figure S32. HMQC spectra of complex **6** in DMSO-d_6.

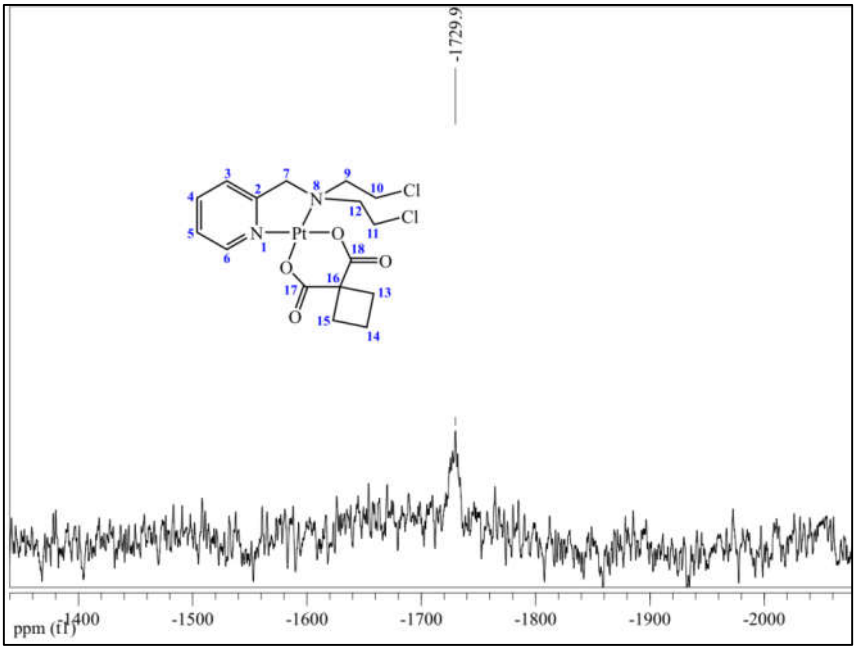

Figure S33. ^{195}Pt NMR spectra of complex **6** in DMSO-d_6.